

Optical properties of PbTe doped with Nd

M. V. Nikolic · K. M. Paraskevopoulos · T. Ivetić · T. T. Zorba ·
S. S. Vujatovic · E. Pavlidou · V. Blagojevic · A. Bojicic ·
O. S. Aleksic · N. Nikolic · W. König · P. M. Nikolic

Received: 28 December 2009 / Accepted: 28 May 2010 / Published online: 11 June 2010
© Springer Science+Business Media, LLC 2010

Abstract Single crystals of lead telluride doped with Nd were synthesized using the Bridgeman method. Room temperature far infrared reflectivity spectra were measured for PbTe samples with Nd content in the range 0.2–0.9 at.%. Optical reflectivity in the far infrared range was measured in the temperature range between 10 and 300 K for a highly polished PbTe sample with 0.6 at.% Nd. The experimental diagrams were numerically analyzed with a fitting procedure using a modified plasmon–phonon model. Two local modes were noted and their origin was discussed. Optical electron mobility was calculated for all analyzed samples.

Introduction

Lead telluride is a well-known narrow band gap semiconductor used mainly for the production of lasers, infrared

detectors [1], and even thermoelectric devices [2]. Transport and optical properties of PbTe depend on the deep-defect electronic states in the neighborhood of the band gap [3]. Doping PbTe with different impurities has resulted in diverse effects. Extensive experimental and theoretical studies have been conducted of PbTe doped with group-III elements, such as In, Ga, B, or Tl [3–6]. Doping with In or Ga lead to the Fermi-level pinning effect and the persistent photo-conductivity effect or in the case of Tl superconductivity [3, 6]. Other dopants, such as transition metals Mn, Cr, Ni, and Fe [7–10] have also been studied. Physical properties and possible applications of lead telluride doped with rare earth elements are the subject of many current studies [11, 12]. When some lead ions are substituted with paramagnetic ions (like for example, Eu²⁺, Gd²⁺, Yb²⁺) IV–VI semiconducting compounds (PbTe, PbSe, etc.) become diluted magnetic semiconductors (known also as semimagnetic semiconductors) [13–15]. Lead telluride doped with rare earth metals exist in the NaCl face centered cubic crystal structure that is the same structure as pure PbTe. For rare earth impurities the energy of electronic states depends primarily on the Coulomb interaction between the *f* electrons of the solute [16]. The mixed valence behavior of the dopant is dependent on the energy gap and the Fermi level position depends on the carrier density. Weaker coupling between solute and host states could have a significant effect on the valence state of the rare earth impurity if the energies of corresponding energy states are low.

Far infrared properties of PbTe doped with Sm [17], Ce [18], Yb [19], and Gd [20] were recently examined in the temperature range 10–300 K. The dopant concentration of Sm and Ce was 0.5 at.%. The determined room temperature optical mobility of free electrons increased with decreasing amount of dopant and thus was about

M. V. Nikolic · O. S. Aleksic · N. Nikolic
Institute for Multidisciplinary Research, Kneza Višeslava 1,
11000 Belgrade, Serbia

K. M. Paraskevopoulos · T. T. Zorba · E. Pavlidou
Physics Department, Solid State Section, Aristotle University
of Thessaloniki, 54124 Thessaloniki, Greece

T. Ivetić · S. S. Vujatovic · A. Bojicic · P. M. Nikolic (✉)
Institute of Technical Sciences of SASA, Knez Mihailova 35/IV,
11000 Belgrade, Serbia
e-mail: pantelija.nikolic@sanu.ac.rs

V. Blagojevic
Faculty of Electrical Engineering, University of Belgrade,
Bulevar Kralja Aleksandra 73, 11000 Belgrade, Serbia

W. König
Max Planck Institut für Festkörperforschung, Heisenbergstrasse
1, 7000 Stuttgart 80, Germany

$7200 \text{ cm}^2/\text{V s}$ for $\text{PbTe} + 0.2 \text{ at.\% Yb}$ and $2400 \text{ cm}^2/\text{V s}$ for $\text{PbTe} + 0.5 \text{ at.\% Yb}$ [19]. Thus, smaller amounts of dopant could be expected to result in increased free electron/hole mobility in the resulting sample. Alekseeva et al. [12] also noted higher values of free electron mobility for smaller dopant concentrations, though they investigated the range $0.5\text{--}1 \text{ at.\% La and Pr}$, 2 at.\% Gd , and 5 at.\% Sm . In the literature, it was shown that the optimal concentration of Cr in PbTe was 0.2 at.\% [8] and also for Ga in PbSnTe [4]. We also obtained high free electron mobility values for 0.2 at.\% of Fe [10] and Gd [20] in PbTe.

In the present paper far infrared spectra for PbTe doped with $0.2\text{--}0.9 \text{ at.\% Nd}$ were measured and numerically analyzed.

Experimental procedure

Single crystal ingots of PbTe doped with the starting composition of 2 at.\% Nd were grown using the standard Bridgman method [21]. High purity elements (6 N) were used as the source material. Samples were cut or cleaved from the ingot and then highly polished before they were used for measurements. X-ray diffraction analysis of samples proved they were single crystal. The content of Pb, Te, and Nd in each sample was determined using EDS analysis. Along the ingot, the concentration of Nd increased from the top to the end of the ingot. This enabled cutting of samples with different contents of Nd. Far infrared reflectivity spectra of a PbTe sample doped with 0.6 at.\% Nd were measured in the temperature range between 10 K and room temperature using a Bruker IFS-113V spectrometer equipped with an Oxford Instruments cryostat. Room temperature far infrared reflectivity spectra were measured on PbTe samples with Nd content in the range $0.2\text{--}0.9 \text{ at.\%}$. All samples were determined to be of the n-type.

Experimental results and discussion

The measured far infrared spectra of single crystal PbTe doped with 0.6 at.\% Nd in the temperature interval $10\text{--}300 \text{ K}$ are shown in Fig. 1. A relatively sharp dip at wave numbers between 150 and 180 cm^{-1} was observed for each temperature. It is less pronounced only for room temperature. For that temperature, the plasma minimum is at the lowest wave number and it gradually moves toward higher wave numbers when the temperature decreases. A peak at about 220 cm^{-1} was observed for the reflectivity spectra measured at 10 K . With increasing temperature, it became less noticeable and it was still clearly observed at about 213 cm^{-1} for the reflectivity spectra measured at 110 K . This peak is regarded as a local impurity mode.

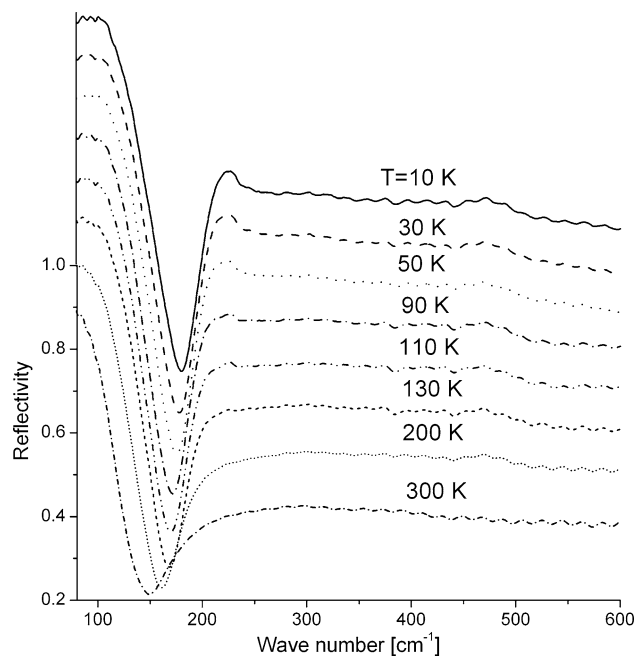


Fig. 1 Reflectivity spectra of $\text{PbTe} + 0.6 \text{ at.\% Nd}$ at temperatures between 10 and 300 K

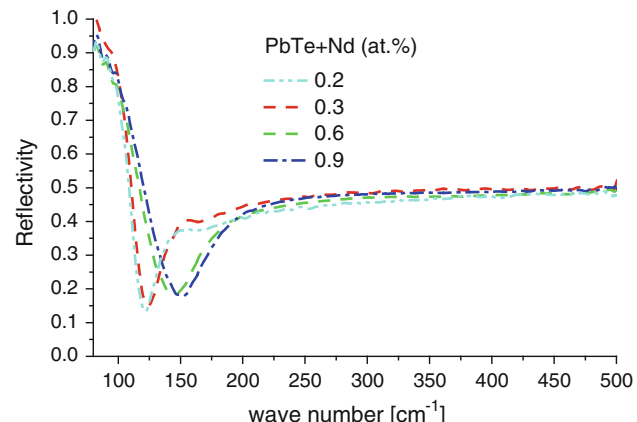


Fig. 2 FIR spectra of PbTe doped with $0.2\text{--}0.9 \text{ at.\% Nd}$ measured at 300 K

Figure 2 shows measured room temperature infrared spectra of single crystal PbTe doped with $0.2\text{--}0.9 \text{ at.\% Nd}$. For lower Nd concentrations (in the range $0.2\text{--}0.3 \text{ at.\%}$), the plasma minimum has shifted to lower frequencies of around 120 cm^{-1} and another local mode can be noted at about 150 cm^{-1} , that was not noticeable for samples with Nd content in the range $0.5\text{--}0.9 \text{ at.\%}$ as their plasma minimum was in the range $144\text{--}150 \text{ cm}^{-1}$.

All experimental results were numerically analyzed using a modified four parameter model for the dielectric function [22] which takes into account that in our case the pure longitudinal-LO modes of the lattice are strongly

Table 1 Calculated optical parameters for PbTe doped with 0.6 at.% Nd in the temperature range 10–300 K and PbTe doped with 0.2 at.% Nd (all values except T , K and ε_{∞} are given in cm^{-1})

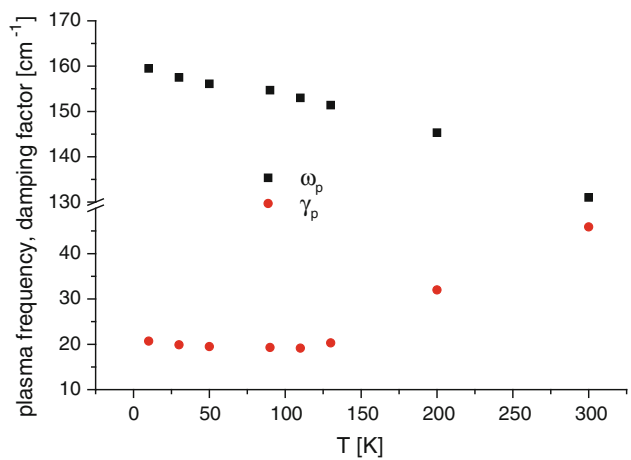
T :	0.6 at.% Nd								0.2 at.% Nd
	10	30	50	90	110	130	200	300	300
ω_{01}	145.0	145.0	145.0	145.0	145.0	145.0	145.0	145.6	144.7
γ_{01}	2153	1414	1758	1276	808	692	965	968	26
ω_{L1}	175.0	176.0	173.0	170.0	167.0	164.0	157.0	139.0	148.0
γ_{L1}	141	140	153	145	145	134	132	175	48
ω_{02}	220	219	217	214	213.4	212.7	209	207	207
γ_{02}	19.8	22.7	24.7	26.7	34.2	38.0	57.6	13.9	419.7
ω_{L2}	227.5	227	227	227.5	227	227	227	227.5	227.6
γ_{L2}	136	138	131.6	118.2	119	124	151	400	603.8
ε_{∞}	33.0	32.6	32.0	31.6	31.0	31.0	30.5	30.0	30.5

influenced by the plasma mode of the free carriers [23]. Details of this modified model are given in our previous work [17, 19]. The values of some calculated optical parameters are given in Table 1 for two Nd concentrations in PbTe, 0.2 at.% at room temperature (300 K) and 0.6 at.% in the temperature range 10–300 K. The impurity local modes are denoted as ω_{01} and ω_{02} and ω_{L1} , ω_{L2} are their longitudinal optical modes; γ_{01} , γ_{02} , γ_{L1} , γ_{L2} are their damping factors, respectively and ε_{∞} is the high frequency dielectric permittivity. One can see that at room temperature the damping factors for the two local impurity modes differ for the two different Nd concentrations, i.e., the lower frequency mode at about 145 cm^{-1} has much lower damping factors for the Nd concentration of 0.2 at.% where this mode is noticeable in the measured diagram than for the Nd concentration of 0.6 at.% where this mode is obscured by the plasma minimum. The higher frequency local mode at about 207 cm^{-1} was most clearly noted at 10 K (Fig. 1), and its damping factors are higher for the Nd concentration of 0.2 at.%. Table 2 gives determined values from room temperature far infrared spectra for the plasma frequency ω_p and μ_n optical mobility of the majority free carriers for different Nd concentrations. The optical electron mobility was calculated using reflectivity diagrams and the method of Moss et al. [24]. One can see that the calculated plasma frequency value is somewhat lower for lower Nd concentrations. This is in accordance with

previously noted changes in the position of plasma minimum for samples doped with 0.5 and 0.2 at.% Yb, where the plasma minimum decreased from 160 to 120 cm^{-1} [19]. Similarly, the determined optical electron mobility values increase for lower Nd concentrations starting with $1940 \text{ cm}^2/\text{V s}$ for 0.9 at.% Nd to 6520 for 0.2 at.% Nd. The calculated values for the plasma frequency ω_p and damping factor γ_p for PbTe + 0.6 at.% Nd versus temperature are given in Fig. 3. The damping factor is about 20 cm^{-1} at 10 K and decreases when the temperature increases reaching 19.15 cm^{-1} at 110 K and then increases with temperature reaching about 40 cm^{-1} at 300 K. Such a change of γ_p was also noted for PbTe samples doped with Yb [19] and Ga [5] where the persistent photoconductivity effect was registered. The critical temperature, where the damping factor starts to increase with temperature, in our case is $T_c \approx 110 \text{ K}$. In Fig. 4, the change of optical mobility of free carriers in PbTe doped with 0.6 at.% Nd is given versus the temperature. It is the highest at low

Table 2 Plasma frequency and free carrier optical electron mobility for n-type PbTe doped with 0.2–0.9 at.% Nd

Dopant concentration, at.%	ω_p, cm^{-1}	$\mu_n, \text{cm}^2/\text{V s}$
0.2	112	6519
0.3	113	6340
0.6	131	2648
0.9	143	1940

**Fig. 3** Change of plasma frequency and damping factor as a function of temperature for PbTe doped with 0.6 at.% Nd

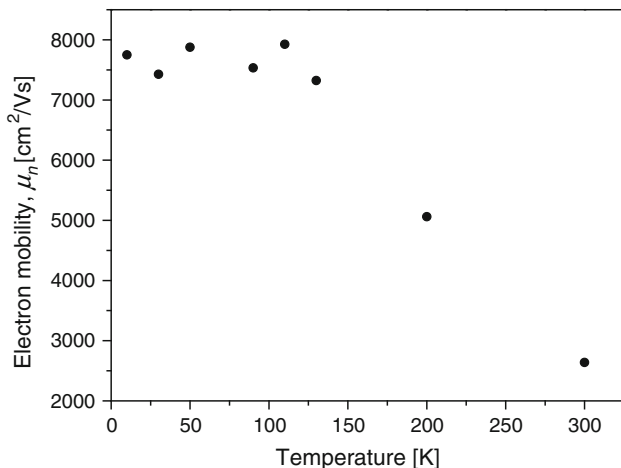


Fig. 4 Change of free carrier optical electron mobility versus temperature for PbTe doped with 0.6 at.% Nd

temperatures, about $7800 \text{ cm}^2/\text{V s}$, reaching a maximum of $7900 \text{ cm}^2/\text{V s}$ at 110 K. Then, it starts to decrease down to $2638 \text{ cm}^2/\text{V s}$ at room temperature when the temperature increases. This value is high compared to the room temperature value for pure single crystal PbTe ($1730 \text{ cm}^2/\text{V s}$) [25]. In Table 2, one can see that for PbTe doped with 0.2 at.% Nd at room temperature the optical mobility is $6519 \text{ cm}^2/\text{V s}$, almost four times higher than for pure PbTe. This is similar to the value obtained when PbTe was doped with 0.2 at.% Yb [19].

Thus, doping with rare earth elements improves the free carrier mobility of PbTe, relatively low amounts of dopant need to be used and they vary depending on the element used. The optimal concentration is about 0.2 at.%. A similar conclusion was made when PbTe was doped with Ga [4] and even Cr [8].

Two local modes for n-type PbTe doped with different rare earth elements were observed in this work for Nd, and in previous work for Yb [19], Gd [20], and p-type PbTe doped with Sm [17] and Ce [18]. Two charge states were also noted for Yb in PbTe from two-photon absorption measurements [26], EPR [27] and magnetic measurements [28]. Knowing that Nd-like Ce and Yb has two electrons in 5s and 6s shells and six electrons in the 5p shell according to Samsonov [25] the source of ionization of Nd is $4f^46s^2$ (5J_4) with ionized states $e^{1+}-4F^46s$ ($^6J_{7/2}$); $e^{2+}-4f^4$ (5J_4) and $e^{3+}-4f^3$ ($^4J_{9/2}$). In [28], it was shown that a smaller fraction of Yb in the magnetically active charge state Yb^{3+} with most Yb ions in the nonmagnetic Yb^{2+} state were present in p-type $Pb_{1-y}Yb_yTe$ (y ranged between 0.03 and 6.5 mol.%). In our case, the dopant concentrations are low, so we can expect rare earth ions in both valence states. Though not so common, mixed valence of Nd has been noted [29]. Thus, Nd enters the PbTe lattice in two charge states: neutral ($^{2+}$) and as a donor ($^{3+}$). The lower

frequency local mode is assigned to the ion in the neutral charge state ($^{2+}$), while the higher frequency local mode is assigned to the donor charge state ($^{3+}$). In the case of PbTe doped with 0.6 at.% Nd the Nd^{2+} local mode was stable at low temperatures (calculated to be at 145 in the range 10–200 K and very slightly higher—145.6 at room temperature), while the Nd^{3+} local mode shifted from 207 to 220 cm^{-1} in the temperature range between 300 and 10 K. Similar changes were noted for n-type PbTe doped with 0.5 at.% Yb [19] where the assigned Yb^{2+} local mode was stable at 156 cm^{-1} in the temperature range 10–300 K and it did not change for lower Yb concentration. The mode assigned to Yb^{3+} shifted from 247.5 to 297.8 in the temperature range 300–10 K [19]. This shift in modes at low temperatures was not noted for p-type PbTe doped with 0.5 at.% Sm [17] and 0.5 at.% Ce [18].

Doping PbTe with group-III elements such as In or Ga leads to the Fermi-level pinning effect. Formation of analogous impurity states was noted for PbTe doped with Yb [26] where this rare earth element substituted Pb^{2+} ions. While for In the Fermi-level pinning effect results from valence switching between In^+ and In^{3+} , this is not the case for rare earth elements. EPR data have shown that Fermi level pinning in the case of doping with rare earth elements, such as Yb or Gd occurred as switching of the impurity valence, i.e., $Yb^{2+}-Yb^{3+}$ [14, 20, 27]. Also, the position of the pinned Fermi level did not depend on dopant concentration of the group-III element (In), but in the case of Yb (rare earth element) the Fermi-level strongly depended on the dopant concentration [7]. For low dopant concentrations (Yb), the Fermi-level was pinned below the top of the valence band. In p-type $Pb_{1-y}Yb_yTe$ [27], the free hole concentration and mobility depended strongly on the alloy composition, i.e., the amount of dopant used. For lower dopant concentrations, the Fermi level was noted about 40 meV below the valence band edge, with increased dopant concentrations it shifted toward the valence band edge [27]. This was explained by the formation of a resonant impurity level that depends on the dopant concentration. For low dopant concentrations filling of the valence band take place, due to the donor activity of the rare earth element (Yb), thus a fraction of Yb ions is in the Yb^{3+} charge state until the Fermi level is pinned by the impurity level. Higher dopant concentrations lead to movement of the impurity level into the forbidden band and increase in the concentration of native defects. Acceptor activity of these native point defects compensates for donor activity of the dopant element, but the rate of native defect formation did not follow the rate of increase in Yb concentration. Thus, for higher Yb concentrations most Yb ions were present in the neutral, nonmagnetic Yb^{2+} state.

Thus, for the studied very low concentration of rare earth impurities in PbTe and their donor-like behavior in

PbTe [12] one can say that impurity atoms first fill the vacancies of Pb in the lattice. Optical reflectivity measurements can register local impurity modes whose position, among other things, depends on the type of impurity element, the dopant concentration and the impurity center charge. The theory of mixed valence state in PbTe narrow gap semiconductors might take into account better the peculiarities of the wave functions and energy spectrum of this compound doped with rare earth elements [16]. Anharmonic electron phonon interactions could be considered to play a principal role in PbTe doped with rare earth elements [30]. These interactions near low temperature phase transformations in semiconductors could be investigated using third-order nonlinear optical methods [26].

Conclusion

In this work, far infrared reflectivity spectra of n-type PbTe doped with 0.6 at.% Nd were measured in the temperature range between 10 and 300 K and numerically analyzed. A strong plasmon–phonon interaction was observed and also two impurity local modes—one stable at 145 cm^{-1} and the second at 207 cm^{-1} at room temperature increased to about 220 cm^{-1} at 10 K. Room temperature far infrared reflectivity spectra were measured of PbTe samples with 0.2–0.9 at.% Nd.

Two local modes were noted in all samples. The determined values of optical electron mobility of free carriers for all samples were high compared to pure PbTe. They depended on the rare element concentration. The highest values were obtained for the dopant concentration of 0.2 at.%. This means that PbTe doped with an optimal concentration of rare earth can be used for making infrared devices in modern astronomy with improved characteristics.

Acknowledgements This work was performed as part of project F130 of the Serbian Academy of Sciences and Arts and Project 142011G financed by the Ministry of Science and Technological Development of the Republic of Serbia.

References

- Schiessl UP, John J, McCann PJ (2004) In: Choi HK (ed) Long wavelength infrared semiconductor laser. John Wiley and Sons Inc, New York
- Dresselhaus MS, Lin MY, Koga T, Cronin SB, Rabin O, Black MR, Dresselhaus G (2001) In: Tritt TM (ed) Semiconductors and semimetals: recent trends in thermoelectric research III. Acad. Press, San Diego, CA
- Hoang K, Mahanti SD, Jena P (2007) Phys Rev B 76:115432
- Skipetrov EP, Zvereva EA, Dmitriev NN, Golubev AV, Slynko VE (2006) Semiconductors 40:893
- Romčević N, Romčević M, Khokhlov DR, Belogorokhov AI, Ivanchik II, König W (1999) Infrared Phys Technol 40:453
- Ivanchik I, Khokhlov DR, Belogorkhov AI, Popović Z, Romčević N (1998) Semiconductors 32:608
- Ivanchik II, Khokhlov DR, Morozov AV, Terekhov AA, Slyn'ko EI, Slyn'ko VI, de Visser A, Dobrowolski WD (2000) Phys Rev B 61:R14889
- Akimov BA, Verteletski P, Zlomanov VP, Ryabova LI, Tananaeva OI, Shirokova NA (1989) Sov Phys Semicond 23:151
- Romčević N, Trajić J, Kuznetsova TA, Romčević M, Hadžić B, Khokhlov DR (2007) J Alloys Compd 442:324
- Nikolic PM, Lukovic D, Konig W, Nikolic MV, Blagojevic V, Vujatovic SS, Savic S, Stamenovic B (2008) J Optoelectron Adv Mater 10:145
- Partin DL (1985) J Appl Phys 57:1997
- Alekseeva GT, Vedernikov MV, Gurieva EA, Konstantinov PP, Prokof'eva LV, Ravich YuI (1998) Semiconductors 32:716
- Nouneh K, Plucinski KJ, Bakasse M, Kityk IV (2007) J Mater Sci 42:6847. doi:[10.1007/s10853-006-1331-x](https://doi.org/10.1007/s10853-006-1331-x)
- Zayachuk DM, Kempnyk VI, Bednarski W, Waplak S (1999) J Magn Magn Mater 191:207
- Zlatanov ZK (2007) Mater Chem Phys 103:470
- Dugaev VK, Litvinov VI, Lusakowski A (1999) Phys Rev B 59:15190
- Nikolić PM, König W, Luković D, Savić S, Vujatović S, Radulović K, Blagojević V (2004) J Optoelectron Adv Mater 6:811
- Nikolić PM, König W, Vujatović SS, Blagojević V, Luković D, Savić S, Radulović K, Urošević D, Nikolić MV (2007) J Alloys Compd 433:292
- Nikolić PM, Luković D, Vujatović SS, Paraskevopoulos KM, Nikolić MV, Blagojević V, Zorba TT, Stamenović B, König W (2008) J Alloys Compd 466:319
- Nikolic PM, Paraskevopoulos KM, Vujatovic SS, Nikolic MV, Bojicic A, Zorba TT, Stamenovic B, Blagojevic V, Jovic M, Dasic M, Konig W (2008) Mater Chem Phys 112:496
- Akimov BA, Nikorich AB, Ryabova LI, Shirokova NA (1989) Fiz Tekh Poluprovodn 23:1019
- Gervais F, Piriou B (1974) Phys Rev B 10:1642
- Kukharskii AA (1973) Solid State Commun 13:1761
- Moss TS, Hawkins TDF, Burrell GJ (1968) J Phys C 1:1435
- Samsonov GV (ed) (1976) Properties of elements. Part 1. Physical Properties Metallurgiya, Moscow
- Nouneh K, Kityk IV, Viennois R, Benet S, Charar S, Paschen S, Ozga K (2006) Phys Rev B 73:035329
- Isber S, Charar S, Gratens X, Fau C, Averous M, Misra SK, Golacki Z (1996) Phys Rev B 54:7634
- Skipetrov EP, Chernova NA, Skipetrova LA, Slyn'ko EI (2002) Mater Sci Eng B 91–92:412
- Rodriguez-Betancourt VM, Nattland D (2005) Phys Chem Chem Phys 7:173
- Nouneh K, Kityk IV, Viennois R, Benet S, Plucinski KJ, Charar S, Golacki Z, Paschen S (2005) J Phys D Appl Phys 38:965